JACS Au
AN OPEN ACCESS JOURNAL OF THE AMERICAN CHEMICAL SOCIETY

pubs.acs.org/jacsau

Article

First-Principles Prediction of the Electrochemical Stability and Reaction Mechanisms of Solid-State Electrolytes

Tammo K. Schwietert, Alexandros Vasileiadis, and Marnix Wagemaker*

Cite This: *JACS Au* 2021, 1, 1488–1496

Read Online

ACCESS | Metrics & More | Article Recommendations | Supporting Information

ABSTRACT: Solid-state batteries have significant advantages over conventional liquid batteries, providing improved safety, design freedom, and potentially reaching higher power and energy densities. The major obstacle in the commercial realization of solid-state batteries is the high resistance at the interfaces. To overcome this bottleneck, it is essential to achieve an in-depth fundamental understanding of the crucial electrochemical processes at the interface. Conventional electrochemical stability calculations for solid electrolytes, determining the formation energy toward the energetically favorable decomposition products, often underestimate the stability window because kinetics are not included. In this work, we introduce a computational scheme that takes the redox-activity of the solid electrolytes into account in calculating the electrochemical stability, and it in many cases appears to dictate the electrochemical stability. This methodology is applied to different chemical and structural classes of solid electrolytes, exhibiting excellent agreement with experimentally observed electrochemical stability. In contrast with current perception, the results suggest that the electrochemical stability of solid electrolytes is not always determined by the decomposition products but often originates from the intrinsic stability of the material itself. The processes occurring outside the stability window can lead toward phase separation or solid solution depending on the reaction mechanism of the material. These newly gained insights provide better predictions of the practical voltage ranges and structural stabilities of solid electrolytes, guiding solid-state batteries toward better interfaces and material design.

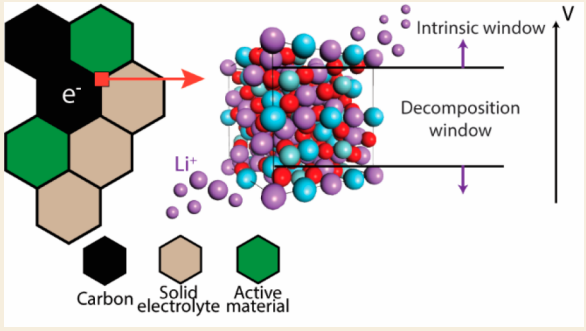

KEYWORDS: *solid-state batteries, solid electrolytes, electrochemical stability, solid electrolyte redox, decomposition window*

INTRODUCTION

Solid-state batteries have received growing interest during the last decades because of their improved safety and potentially superior battery performance. The essential requirements for solid electrolytes are high ionic and low electronic conductivity while maintaining chemical and electrochemical stability at the anode and cathode interfaces during cycling. Several promising inorganic solid electrolytes from different material classes have been developed that exhibit high ionic conductivities. The most intensively investigated solid electrolyte structures include sulfur-based thiophosphates and thio-LISICON conductors (1×10^{-2} to 1×10^{-3} S cm^{-1}), and oxide-based solid electrolytes such as garnets, NASICONs, perovskite, LISICON (1×10^{-2} to 1×10^{-6} S cm^{-1}), and recently, halides.[1−4]

Besides the rapid development of solid electrolytes with high bulk Li-ion conductivities, reaching values even beyond that of liquid electrolytes, interfacial resistance between the solid electrolyte and electrode typically remains the main limiting factor in solid-state batteries.[1−5] The origin of this can include mechanical failure leading to contact loss, space-charge layers, and chemical and electrochemical instability of the solid electrolyte electrode interface.[6] Numerous interfacial strategies have been developed to increase battery performance, but capacity retention and lower rate capability due to parasitic interface processes remain the challenge for solid-state batteries.[3,6] These processes are complex and challenging to study experimentally, and better theoretical understanding of the electrochemical stability of solid electrolytes is a prerequisite.[3,5,6]

More insights into the electrochemical stability window of solid electrolytes and its relationship with the decomposition mechanism have been recently obtained. For several solid electrolytes, it has been shown that cyclic (CV) experiments overestimate the actual electrochemical stability window,[7,8] whereas the prediction of the thermodynamic formation energy of the decomposition products[7−9] often underestimates the actual electrochemical stability window. CV experiments do not capture the electrochemical stability window accurately

Received: May 22, 2021
Published: August 16, 2021

Table 1. Investigated Solid Electrolytes, Including the Redox Element(s) on Oxidation and Reduction and the Theoretical Capacities Associated with Decomposition

material	acronym	redox element oxidation	ox. capacity (mAh/g)	redox element reduction	red. capacity (mAh/g)
Li_3PS_4	LPS	S^{2-}	96.23	P^{5+}	1190.78
Li_6PS_5Br	LPSB	S^{2-}/Br^-	514.01	P^{5+}	685.35
Li_6PS_5Cl	LPSC	S^{2-}/Cl^-	599.14	P^{5+}	798.85
$Li_{10}GeP_2S_{12}$	LGPS	S^{2-}	455.20	P^{5+}/Ge^{4+}	1081.11
$LiBH_4$	LBH	B^{5-}	1230.55	H^+	4922.22
Li_3YBr_6	LYB	Br^-	136.48	Y^{3+}	136.48
Li_3OCl	LOC	O^{2-}/Cl^-	1112.40		
Li_2PO_2N	LIPON	N^{3-} / O^{2-}	589.95	P^{5+}	2359.80
$Li_7La_3Zr_2O_{12}$	LLZO	O^{2-}	223.41	Zr^{4+}/ La^{3+}	255.33
$Li_{0.33}La_{0.56}TiO_3$	LLTO	O^{2-}	50.27	Ti^{4+}/La^{3+}	559.03
$Li_{1.5}Al_{0.5}Ti_{1.5}(PO_4)_3$	LATP	O^{2-}	105.62	P^{5+}/Al^{3+} / Ti^{4+}	2147.69
$Li_{1.5}Al_{0.5}Ge_{1.5}(PO_4)_3$	LAGP	O^{2-}	96.23	$Ge^{4+}/P^{5+}/Al^{3+}$	1812.34

because of the small electrolyte−electrode contact area and the short time scale of these experiments compared to low-current-density solid-state battery cycling.[10] On the other hand, the electrochemical stability window's prediction from formation energies of the decomposition products may underestimate the electrochemical stability window due to the inability of capturing the reaction mechanism and the associated reaction energy barrier toward the decomposition products, which will kinetically hinder the decomposition.

Recently, it was shown that the oxidation and reduction of several solid electrolytes, associated with delithiation and lithiation, respectively, may provide an indirect redox route, via metastable solid electrolyte composition(s), toward the most stable decomposition.[7] In this case, the solid electrolyte acts as an active material (Li source or sink), where the associated anodic or cathodic potential determines the thermodynamic electrochemical stability window. This is only possible if the solid electrolyte is in contact with the electron-conducting network of the electrode, which can be expected to apply for the solid electrolyte material near the anode/cathode and/or near the conductive additive, where the definition of vicinity depends on the electronic conductivity of the solid electrolyte and its decomposition products, which is receiving increasing attention because of its impact on dendrite formation and decomposition.[7,10−12] For the few solid electrolytes investigated, the in-this-way predicted indirect electrochemical stability window was shown to be wider than that associated with direct decomposition, matching the actual electrochemical stability window at small currents (approaching thermodynamic conditions) and supporting this indirect decomposition mechanism, which could also be qualified as kinetic stabilization.[7]

Herein, we extend and deepen this approach by predicting the electrochemical window associated with oxidation and reduction reactions (delithiation and lithiation, respectively) of the most intensively studied solid electrolytes by evaluating solid electrolyte formation energies determined by density functional theory (DFT) calculations. Redox potentials for Li insertion and extraction are calculated and compared to the potentials of direct decomposition toward the most stable chemical products. The results are in good agreement with reported experimental electrochemical stability windows, predicting that the decomposition route typically proceeds via (de)lithiation of the solid electrolyte and that this indirect decomposition mechanism determines the electrochemical stability window of most solid electrolytes. In general, this results in a wider stability window than that calculated on the basis of the stability of the decomposition products, which can be rationalized by a potentially large reaction barrier for decomposition. The results are correlated to different structural responses of the solid electrolyte material to specific potentials, providing fundamental and practical insights into the structural and electrochemical stability of solid-state electrolytes.

METHODS

Density functional theory (DFT) using the Perdew−Burke−Ernzerhof (PBE) generalized gradient approximation (GGA) was applied to determine the lowest energy configurations of (de)lithiated materials.[13] Projected augmented wave (PAW) pseudopotentials as implemented within the *Vienna Ab initio Software Package* (*VASP*)[14] are used. The *k*-point mesh and energy cutoff values for different materials are reported in Table S1. All DFT calculations are performed charge-neutral, taking the oxidation and reduction of the material itself as typically performed for electrode materials.[15]

To determine the configurations of (de)lithiated structures, the following scheme is applied. The lowest static electrostatic energy configurations are generated by minimizing the coulumbic interactions for Li. The above calculation is performed for 10 000 random configurations at each specific Li concentration in a material. Subsequently, for the 10 lowest energy structures, DFT relaxation is performed to obtain the final total energy and structure. To evaluate if there are energetically preferred symmetric sites for delithiation, we also evaluated Li concentrations at different Wyckoff positions. The sites where Li atoms are inserted in the materials are given in Table S1. Structures and formation energies used as references are obtained from the Materials Project.[16]

RESULTS

The solid electrolytes studied are listed in Table 1. Sulfides generally possess a high Li conductivity and good processability but have limited electrochemical stability.[3] In this study, Li_3PS_4 (LPS), thio-LISICON $Li_{10}GeP_2S_{12}$ (LGPS), argyrodites Li_6PS_5Cl (LPSC), and Li_6PS_5Br (LPSB) are considered. Next to sulfides, an emerging complex hydride $LiBH_4$ (LBH) and solid halide Li_3YBr_6 (LYB) are investigated. Halides have attained renewed interest through their combination of relatively high oxidative stability with high Li conductivity.[17,18] In addition, solid oxide electrolytes are investigated, which are generally more electrochemically stable but have a lower ionic conductivity compared to sulfides.[2] Specifically, anti-perovskite Li_3OCl (LOC), perovskite $Li_{0.33}La_{0.56}TiO_3$ (LLTO), and Li_2PO_2N (LIPON) are considered.[16,19] Finally, NASICON electrolytes, $Li_{1.5}Al_{0.5}Ge_{1.5}(PO_4)_3$ (LAGP), and

https://doi.org/10.1021/jacsau.1c00228
JACS Au 2021, 1, 1488−1496

$Li_{1.5}Al_{0.5}Ti_{1.5}(PO_4)_3$ (LATP) electrolytes are investigated, which have been shown to have high oxidative stability.[8] More information about the structures used and the details of DFT relaxations are provided in Table S1.

In this study, two electrochemical stability windows are differentiated: (1) The electrochemical stability window, based on the stability of the decomposition products,[8,9] is referred to as the decomposition window. (2) The electrochemical stability window, based on indirect decomposition via (de)lithiation of the solid electrolyte, is referred to as the intrinsic window.[7] To determine the decomposition window, we calculated the formation energy of the most favorable decomposition products at a specific potential, which are determined from the Li grand potential phase diagram.[8,9] The decomposition potential closest to the stable solid electrolyte phase defines the reduction and oxidation redox potentials of the window. It is essential to realize that this does not consider the decomposition route, and the associated reaction barrier may lead to an overpotential necessary to form the decomposition products. The intrinsic window of a solid electrolyte is determined from the change in calculated formation energies upon Li insertion and extraction. Thus, the solid electrolyte structure is considered electrochemical active through Li insertion/extraction. The associated average oxidation/reduction potential is calculated by referencing the formation energies to the Li-metal chemical potential similar to intercalation electrodes.[15] These (de)lithiated solid electrolyte phases often have a higher formation energy compared to the most favorable decomposition products (decomposition window) and therefore represent metastable or unstable phases. It is proposed that at a specific lithium composition, these solid electrolyte phases become sufficiently unstable to enable decomposition toward the most stable decomposition products, thus representing an indirect decomposition mechanism.[7] The calculated decomposition electrochemical stability window, assuming direct decomposition toward the most stable decomposition products, and the intrinsic electrochemical stability window, assuming indirect decomposition to the most stable decomposition products via (de)lithiation, of the solid electrolytes in Table 1 are shown in Figure 1 and listed in Table 2.

For the sulfide electrolytes (yellow in Figure 1), the intrinsic window is significantly wider than the decomposition window. This is a consequence of the assumption that direct decomposition is kinetically hindered, resulting in the indirect decomposition via (de)lithiation of the solid electrolyte, effectively resulting in kinetic stabilization of the electrochemical stability window. This assumption is supported by the better agreement of the intrinsic stability window with the experimentally observed electrochemical stability. Considering Li_3PS_4 (LPS), its intrinsic oxidative stability of 2.47 V vs Li/Li^+ is in reasonable agreement with the experimental value of 2.6 V.[20] Likewise, the wider intrinsic window of LGPS amounts to 1.19−2.38 V vs Li/Li^+, matching the experimental stability window of around 1.2−2.5 V vs Li/Li^+.[10,11] It has already been shown that the intrinsic electrochemical stability of argyrodite LPSC agrees very well with experiments,[7] and similarly, there is a good agreement with the experimentally observed oxidation at ∼2.5 V vs Li/Li^+ for LPSB. These experiments were performed without extra external pressure applied after assembling and therefore pressure differences of at most several MPa are expected.[21] This is low compared to the much larger pressures that would theoretically influence the stability

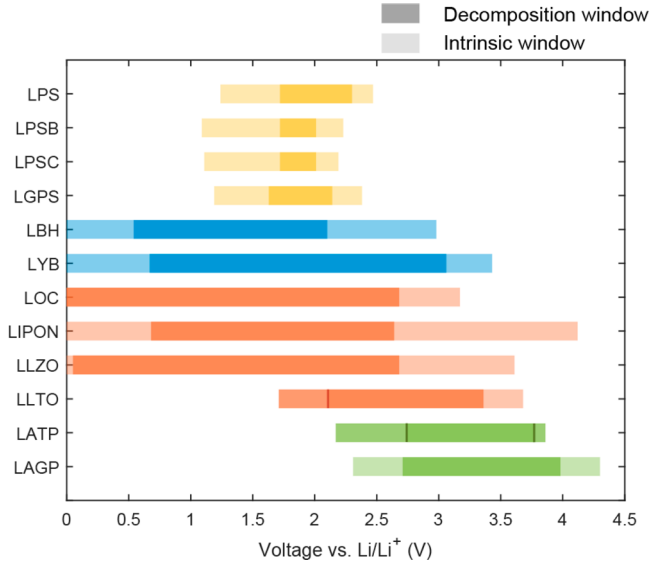

Figure 1. Calculated intrinsic electrochemical stability window and decomposition electrochemical stability window. For most solid electrolytes, the intrinsic oxidation and reduction voltages result in a wider stability window than the decomposition window. However, for LLTO and LATP materials, the intrinsic oxidation/reduction potential is lower/higher than the direct oxidation/reduction, indicated by the solid line.

Table 2. Calculated Decomposition Electrochemical Stability Window, Assuming Direct Decomposition to the Most Stable Decomposition Products (Values in Agreement with the Calculations in Literature[8]), and the Calculated Intrinsic Electrochemical Stability Window Based on the Oxidation and Reduction Potentials for (De)inserting Lithium for Different Solid Electrolytes

material	decomposition ox/red (V)	intrinsic ox/red (V)
LPS	1.72−2.30	1.24−2.47
LPSB	1.72−2.01	1.09−2.23
LPSC	1.72−2.01	1.11−2.19
LGPS	1.63−2.14	1.19−2.38
LBH	0.54−2.10	0.00−3.43
LYB	0.67−3.06	0.00−3.43
LOC	0.00−2.68	0.00−3.17
LIPON	0.68−2.64	0.00−4.12
LLZO	0.05−2.68	0.00−3.61
LLTO	1.71−3.36	2.10−3.68
LATP	2.17−3.86	2.74−3.77
LAGP	2.71−3.98	2.31−4.30

window of solid electrolytes.[22] In the sulfide solid electrolytes, delithiation results in oxidation of S^{2-} toward S^0 around 2.2−2.5 V vs Li/Li^+, as expected, similar to the potential of sulfur electrodes. Upon lithiation, P is reduced from P^{5+} to P^0 around 1.1−1.2 V vs Li/Li^+ and further reduces to P^{3-} (Li_3P) below 0.78 V.[23] We want to clarify again that CV experiments using sulfide solid electrolytes report voltage ranges beyond 0−5;[24,25] however, these experiments are performed without conductive additive mixed with the solid electrolyte and are thus unable to capture the intrinsic electrochemical window.[10]

Similar to sulfide electrolytes, the intrinsic window of lithium boron hydride LBH and halide LYB is significantly larger as compared to the decomposition window. For both solid electrolytes, the indirect reductive potential predicts stability

https://doi.org/10.1021/jacsau.1c00228
JACS Au 2021, 1, 1488−1496

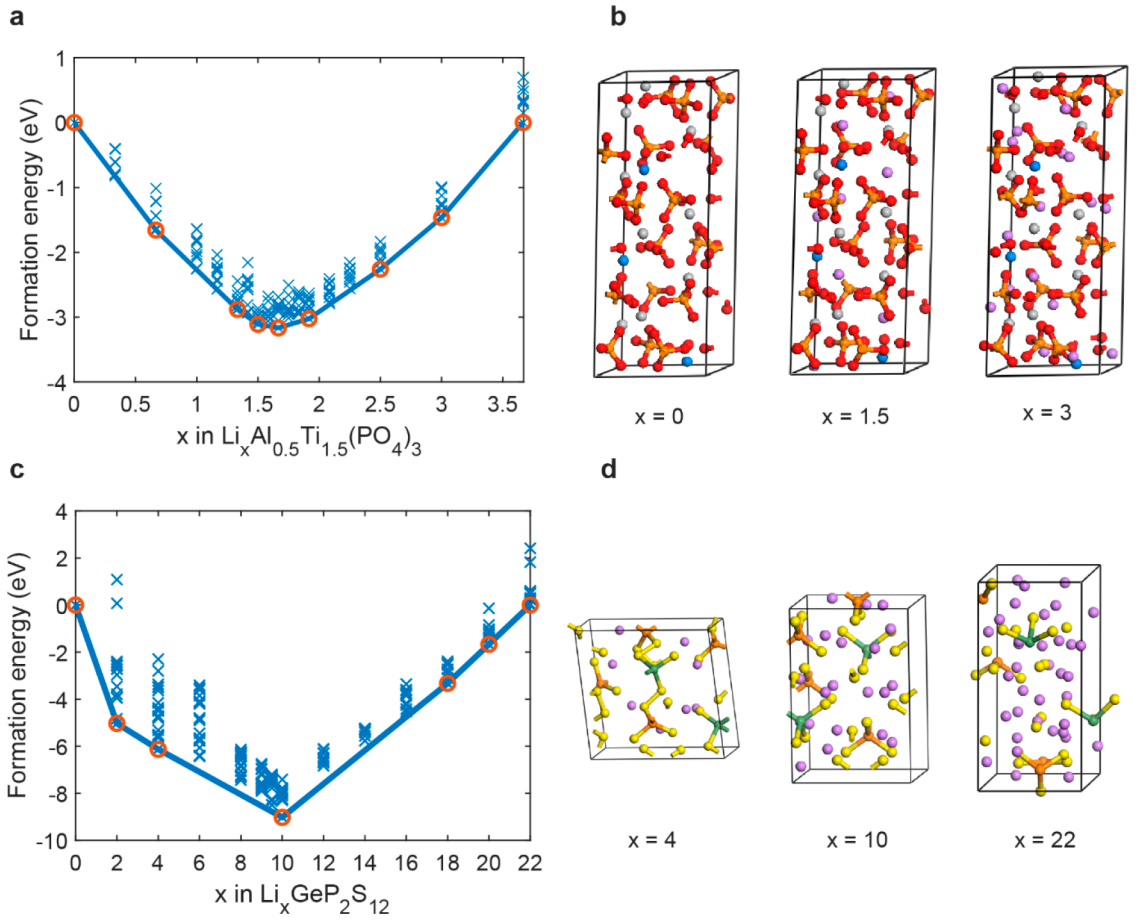

Figure 2. (a) Formation energies per formula unit of $Li_xAl_{0.5}Ti_{1.5}(PO_4)_3$ (LATP) with (b) corresponding structures after DFT relaxations for x = 0, 1.5, and 3. On the convex hull the most stable Li concentrations are shown with an orange circle. Red spheres indicate oxygen, orange phosphorus, white titanium, blue aluminum, and pink lithium. (c) Formation energies of $Li_xGeP_2S_{12}$ (LGPS) with (d) the corresponding structures of x = 4, 10, and 22, where the green sphere indicates germanium and the yellow indicates sulfur. The convex hull of LATP has a convex shape, indicating solid solution behavior for both Li insertion and removal; the corresponding structures for lithiation and complete delithiation appear to be stable after DFT relaxation. For LGPS, the convex is V-shaped between x = 4 and x = 18, indicating phase separation. Further proof is also seen in the corresponding structure after relaxation, where the lattice parameters and angles change, and bonds form and cleave during (de)lithiation of the structure. The convex hulls of the additional solid electrolyte materials are shown in Figures S1−S7.

toward Li metal. Electrochemical stability of the boron hydride has been shown experimentally around 0−3 V vs Li/Li^+,[18] matching the intrinsic stability window calculations. For halide LYB, a relatively high oxidative voltage is predicted (3.43 V), for which in a battery with $LiCoO_2$ as active material, a higher columbic efficiency is achieved compared to sulfur electrolyte LPS.[17] However, at low potentials, LYB is reduced against Li metal, whereas the intrinsic window predicts it is stable toward Li metal. Thus, in this case, the decomposition window has a better predictive value. We propose that this is the consequence of the simple composition built from few elements, thus having a small compositional space, where Li closely surrounds Y and Br in the structure. This can be expected to result in a small nucleation barrier for direct decomposition upon reduction into Y and LiBr, and thus the practical reduction potential approaches that of the predicted decomposition stability window. The large oxidative intrinsic stability window of LBH and LYB can be attributed to the strength of BH_4^- and YBr_6^{3-} backbones in these structures, similar to $NaBH_4$, for which it has been shown that desodiation leads to larger oxidative stability as compared to direct decomposition.[26]

In anti-perovskite Li_3OCl (LOC), where Li is the only element that can be reduced, the reductive decomposition stability equals the Li-metal potential,[8] making it a suitable choice for Li-metal batteries.[3] The intrinsic oxidative stability, 3.17 V vs Li/Li^+, is for this material larger than that predicted by direct decomposition. Accurate oxidation potentials are not reported for LOC. However, the low Coulombic efficiency and formation of decomposition products in combination with $LiCoO_2$ suggest the stability window to be below the $LiCoO_2$ potential.[3] The predicted intrinsic stability window of LIPON, 0.00−4.12 vs Li/Li^+, is significantly larger than the predicted decomposition window, 0.68−2.64 vs Li/Li^+. Consistent with the intrinsic window, it has been shown that LIPON is oxidized around 4.3 V by Put et al.[27] The reductive stability of LIPON against Li metal is disputed, where apparent stability against Li metal is suggested from experiments, and LIPON is even used to coat Li-metal anodes effectively.[3,27−29] Nevertheless, different studies show the reduction of P and N in contact with Li metal.[3,30] Here, intrinsic stability against Li metal is predicted by the convex hull of LIPON, with stable configurations on the convex at Li_1PO_2N and Li_4PO_2N (Figure S6). The compositions just above the convex represent metastable phases that may occur at small overpotentials in

https://doi.org/10.1021/jacsau.1c00228
JACS Au 2021, 1, 1488−1496

practice. Garnet LLZO is predicted to have an oxidation and reduction potential of 0.05 and 2.68 V vs Li/Li^{+}, respectively, assuming direct decomposition. This window is increased to 0−3.61 V vs Li/Li^{+} assuming the intrinsic decomposition. This is in excellent agreement with the observed stability against Li metal and a demonstrated oxidation potential of 3.6 V vs Li/Li^{+} for LLZO.[10,31,32]

The predicted intrinsic stability window is wider than the predicted direct decomposition window for the solid electrolytes discussed so far. Interestingly, for Perovskite LLTO, the direct reduction potential to form the decomposition products is predicted to be lower than the indirect reduction via lithiation of the LLTO structure. This implies that Li-ion insertion in the LLTO structure is energetically more favorable than the formation of decomposition products. Thus lithiation should occur before decomposition. Indeed, intercalation of LLTO has been demonstrated, reflecting the reduction of Ti^{4+} toward Ti^{3+}, similar to, for instance, $Li_4Ti_5O_{12}$ electrodes,[33] demonstrating that the indirect stability window is not always wider than the window predicted based on direct decomposition. The oxidative potential of LLTO is predicted to be larger than that for direct decomposition, and as expected, similar compared to oxide electrolytes.

That the intrinsic window can be smaller than the direct electrochemical stability window is also demonstrated by NASICON type LATP. As shown in Figure 1, LATP has an intrinsic stability window more narrow than its decomposition window, resulting from the lower oxidation potential upon delithiation and higher reduction potential upon lithiation. This reveals that similar to LLTO, Li-ion insertion is predicted to occur before decomposition upon reduction, and Li-ion extraction is predicted to occur before decomposition upon oxidation. In Figure 2a, the many compositions on, or just above the convex hull, both upon lithiation (reduction) and delithiation (oxidation), indicate solid solution reactions in both cases, representing a gradual and homogeneous change in lithium composition in chemical potential, and thus in the oxidation and reduction potentials. Upon reduction, this is supported by experiments, demonstrating that intercalation of $Li_{1+x}Ti_{2-x}Al_x(PO_4)_3$ sets in at 2.5 V vs Li/Li^{+}, which gradually reduces during continuous reduction.[34] Figure 2b displays the structure of LATP ($Li_{1.5}Al_{0.5}Ti_{1.5}(PO_4)_3$) as well as the completely delithiated $Al_{0.5}Ti_{1.5}(PO_4)_3$ and lithiated structures $Li_3Al_{0.5}Ti_{1.5}(PO_4)_3$ (Ti is fully reduced from Ti^{4+} to Ti^{3+}) after DFT relaxation. In the lithiated LATP structure, the rhombohedral lattice remains intact, and only minor reorientations of PO_4 groups can be observed. Similar distortions in symmetry are observed experimentally during the lithiation of LATP, where the reduction of Ti leads to symmetry lowering of the lithiated samples from $R\bar{3}c$ to $R\bar{3}$.[35] During oxidation, where lithium is extracted from the structure, the oxidation voltage toward the first point on the convex hull is 3.37 V. Also, upon delithiation to $Al_{0.5}Ti_{1.5}(PO_4)_3$, structural relaxation indicates that the rhombohedral structure is maintained. Without evaluating the chemical stability of $Al_{0.5}Ti_{1.5}(PO_4)_3$, we anticipate this to be stable on the basis of the predicted chemical stability of rhombohedral $Ti_2(PO_4)_3$ (0.013 eV per atom above the hull).[16] Here, it should be noticed that the supercell size determines the Li-composition step in the convex hull. The intrinsic window limits in Figure 1 and Table 2 are thus artificially defined by the smallest composition step of the supercell considered. These results imply that LATP is electrochemically unstable at a smaller intrinsic window; however, whether the decomposition products form depends on the structural stability and reversibility upon (de)lithiation, similar to what insertion electrodes experience during cycling.

Indeed, structurally reversible lithiation and delithiation have been experimentally shown for LATP, resulting in a gradual change in intercalation potential, consistent with a solid solution reaction.[35] This implies that the structural stability of the solid electrolyte extends beyond the electrochemical stability window. The intrinsic window defines when (de)-lithiation occurs, which generally reduce the Li ion and may increase the electron conductivity depending on the defect formation mechanism of the solid electrolyte, located near the electrode surface where it can be redox active. As a result, a further increase in the internal resistance or promotion of redox activity of the solid electrolyte is expected. LATP has been shown to form structurally stable interfaces beyond its electrochemical window (both decomposition and intrinsic) at high potentials versus an NMC electrode.[36] In contrast to LATP, NASICON LAGP is predicted to have an intrinsic stability window that is wider than the decomposition window, where on both oxidation (delithiation) and reduction (lithiation), a first-order phase transformation is predicted, suggesting the indirect formation of the most stable decomposition products.

The convex hull of sulfide electrolyte LGPS is shown in Figure 2c, between $x = 4$ and $x = 18$, a V-shape is found, indicating on phase separation during oxidation ($x > 10$) and reduction ($x < 10$). In Figure 2d, the structures of the most stable configurations $Li_4GeP_2S_{12}$ and $Li_{18}GeP_2S_{12}$ are shown. In contrast to LATP, large changes in lattice constants and atomic bonds are observed, originating from S^{2-} that is oxidized to S^0 in $Li_4GeP_2S_{12}$ and from Ge^{4+} and P^{5+} that are reduced in $Li_{18}GeP_2S_{12}$. This is confirmed by Figure 2d, where it is shown that structural changes occur; during delithiation, a S−S bond forms in the PS_4 and GeS_4 groups, indicating the oxidation of S^{2-}. Upon lithiation, the P−S and Ge−S bonds break, indicating on the reduction of Ge^{4+} and P^{3+}. These changes in bonds are also reflected in the radial distribution function after relaxation (Figure S9). After reaching the kinetic metastable phases ($Li_4GeP_2S_{12}$ and $Li_{18}GeP_2S_{12}$), the material is expected to transform into the energetically more stable decomposition products, which can also be active during further oxidation and reduction.[7] That the solid electrolyte LGPS is redox active itself and that the oxidation can be attributed to the Li−S within the LGPS structure has been shown experimentally.[11]

The properties of the decomposition products as well as accessible intermediate metastable phases can play an important role in the rate and extent of the decomposition, depending on their electronic[37] and ionic conductivity as well as their volumetric changes.[38] For the decomposition products of several solid electrolyte families, this has been considered elsewhere. Note that the compositions on the convex hull through which the indirect decomposition takes place may be unstable, such that decomposition readily occurs.[7] This implies that the properties of these compositions may not be decisive for the progress of decomposition, but rather the properties of the resulting decomposition products. In case the (de)lithiated phases are stabilized, it is important to evaluate the properties of these metastable (de)lithiated phases that can form upon changing the lithium composition in the solid electrolytes. The volumetric change, band gap, and ionic conductivities of such

https://doi.org/10.1021/jacsau.1c00228
JACS Au 2021, 1, 1488−1496

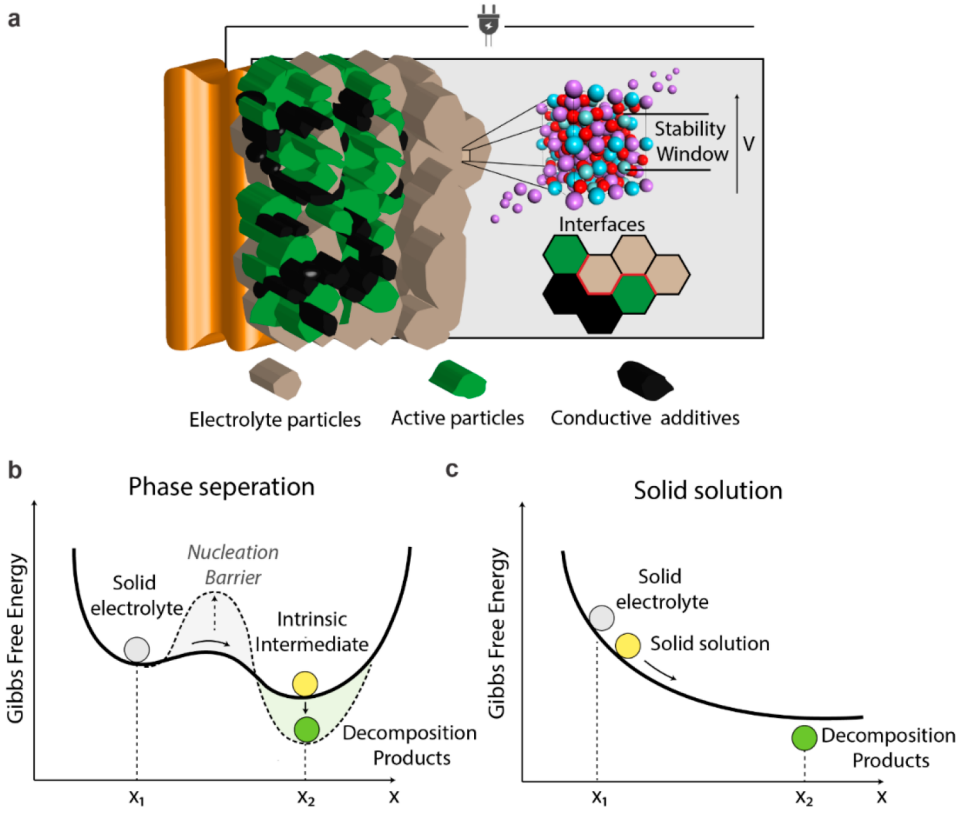

Figure 3. (a) Schematic representation of a solid-state battery, the solid electrolyte is exposed to a potential at the interface with the conductive additive and active electrode particles. (b, c) Schematic energy diagrams versus Li composition in a solid electrolyte for a first-order phase and solid solution reaction. For phase separation, the solid electrolyte generally tends to react toward decomposition products in thermodynamic equilibrium. However, the stability window is determined by the nucleation barrier between the solid electrolyte and the reaction products. The intrinsic intermediate phase has a low energy barrier because the Li-ion mobility facilitates (de)lithiation, whereas the nucleation energy of the decomposition products can be large depending on the compositional and structural complexity of the material. For solid solution materials, the Li (de)insertion potential can be achieved at lower energy than the formation of decomposition products. Accordingly, the materials will react through the Li composition range until the decomposition potential is reached. A flow diagram showing the calculation routes is presented in Figure S8.

metastable compositions for the presented solid electrolytes are calculated and listed in Table S2 and S13. Most metastable phases show a significant volume increase during lithiation and decrease during delithiation. Decrease may lead to contact loss, raising the internal resistance, whereas an increase may hinder decomposition during cycling under volume constrains, effectively widening the electrochemical stability window.[22] The band gaps of the metastable phases generally decrease upon lithiation, as more electrons are inserted in the structure. Although there is no direct relationship between the bandgap and the electronic conductivity, a decreasing bandgap is an indicator for improved electronic conductivity. The composition of most solid electrolytes is optimized toward ionic conductivity, and hence it drops for the (de)lithiated phases as observed in Tables S2 and S13. Nevertheless, they remain ionic conductors, which in combination with increased electronic conductivity will promote the electrochemical decomposition reactions.[6]

DISCUSSION

A schematic solid-state battery is shown in Figure 3a. Good solid−solid contact is required to establish good ionic transport between the electrolyte and active particles. In the vicinity of this contact, the electrolyte is exposed to the applied potential and will decomposes according to its electrochemical stability window. Vicinity is difficult to determine, but it scales with the electronic resistance of the solid electrolyte and time that the electrolyte is exposed to the electrode potential. The decomposition centers related to the (de)lithiation of the electrolyte are enabled by the limited electronic conductivity of the solid electrolyte in a manner that closely resembles the (de)lithiation of electrodes.[37]

For many solid electrolytes, the indirect transformation via (de)lithiation (intrinsic window) predicts a stability window that is wider than that predicted based on the direct transformation into the decomposition products (decomposition window). As an illustration of these transformation routes, Figure 3b, c shows two schematic energy diagram scenario's for (de)lithiation of solid electrolytes. When this initiates a phase transition, the solid electrolyte reaction route goes through the (de)lithiated phase toward the favorable decomposition products. Solid electrolytes have high ionic conductivities and thus, small activation energies are required toward the lithiated and delithiated phases. Thereby the intrinsic metastable phase provides a low barrier indirect pathway toward the decomposition products. In the case of a solid solution transition, Li-ion insertion in the structure will in generally be associated with a low activation barrier as compared to the formation of the decomposition products. In this case, the end of the solid solution reaction is most likely determined by the decomposition potential. The importance of metastable phases in solid electrolytes is already revealed by

https://doi.org/10.1021/jacsau.1c00228
JACS Au 2021, 1, 1488−1496

the intrinsic chemical instability of most solid electrolytes toward decomposition products in thermodynamic equilibrium. The complexity of solid electrolytes varies from simple solids built up by only a few elements (binary salts) up to complex materials built by many elements (e.g., LLZO and LPSB). A larger number of elements in a specific compound, thus representing more complex solids, in general raises the nucleation barrier toward stable decomposition products, thus enabling the formation of intermediate metastable phases.[28] Additionally, the type of bonds, electronic structure, and chemical disorder can contribute to the chemical complexity of a material, further increasing the nucleation barrier toward decomposition. The higher nucleation barrier for these complex materials toward their decomposition products implies that direct composition is kinetically hindered. Therefore, for complex solid electrolytes, it is expected that the direct decomposition stability window is a lower limit and that redox activity will take place at potentials dictated by intrinsic (de)lithiation. Vice versa, materials with a smaller compositional space, e.g., binary Li salts, the nucleation barrier toward direct decomposition can be expected to be smaller (because of the smaller diffusion distances required) and thus the practical stability will approach the electrochemical decomposition window. Solid electrolytes are designed to have low diffusional barriers for Li-ions, facilitating the reaction pathway via intermediate metastable phases, whereas the host structure elements are intended to have a low diffusivity. For example, in the argyrodite Li_6PS_5Br (LPSB) solid electrolyte, low stoichiometric amounts of Br and P make it relatively difficult to form and isolate the LiBr and P decomposition products, rationalizing why the formation energy toward the kinetic stabilization of lithiated metastable phases is more effective. For less complex Li_3YB_6 (LYB), where there are fewer elements in the unit cell, the arranging and formation of decomposition products is expected to be easier, explaining why the actual electrochemical stability window can be smaller than the intrinsic stabilization potential suggest, consistent with the observed decomposition in contact with Li metal.[17]

That solid electrolytes do not directly form the decomposition products, and instead react through intermediate phases has been experimentally observed for various materials. Metastable intermediate phases where sulfur is connected into $P_2S_8^{4-}$ groups and disproportionation to $P_2S_7^{4-}$ and S has been observed for sulfur-based electrolytes.[7,40,41] Similarly, for oxides, it has been shown that metastable phases exist.[39] Materials with phosphate groups are known to form various P−O groups and (amorphous) metastable phases in the Li_2O−P_2O_5 range. Additionally, for oxide LLZO it has been shown that different Zr suboxides exist and are formed during charging.[10] This again rationalizes why the formation energy toward decomposition products is not representative for the actual stability window. The obvious consequence of redox activity due to (de)lithiation of solid electrolytes is generation of additional capacity (Table 1). Irreversible reactions toward decomposition products, directly or indirectly formed, impact the Coulombic efficiency, whereas reversible reactions of metastable intermediates and decomposition products provide reversible capacities.

The relatively good cycling performance for electrolytes that are unstable toward high-voltage cathode materials (>4 V)[25,42] is attributed to the absence or very limited amount of conductive additive in the cathodic mixture in combination with the use of electronically isolating coatings present on the active materials. This rational strategy prevents direct contact between the solid electrolyte and the potential experienced by the electrode, slowing down or even preventing decomposition reactions.

By obtaining a more precise understanding of the realistic electrochemical stability window and corresponding structural responses, new insights can be found in designing more stable interfaces for solid-state batteries. For phase separation materials, improving bond strengths and material complexity play a crucial role in extending the decomposition window as this determines the height of the nucleation barrier toward decomposition and thus the practical electrochemical window. For solid solution materials, the wider structural stability window compared to the electrochemical window opens possibilities for solid electrolytes to have a reversible contribution to a composite electrode's capacity (generally at the expense of a lower local ion conductivity). Although none of the solid electrolytes calculated here covers the entire window of 0−4.5 V vs Li/Li^+ needed to fulfill stability for a typical Li-metal high voltage cathode battery. The different classes of electrolytes inhibit electrochemical stabilities at various potentials where already proposed strategies as multilayer solid electrolyte batteries and guided formation, or artificial SEI could be applied more accurately.[3,8] In this case, however, more interfaces have to be introduced, which could lower the battery performance.

CONCLUSION

A first-principles computational framework is used to calculate the electrochemical stability of materials taking the intrinsic electrochemical window into account. This framework is applied to the most commonly used solid electrolytes in different classes of materials, showing good agreement with experimental data. For most solid electrolytes, a widening of the electrochemical decomposition stability is predicted. However, for electrolytes as LATP and LLTO, insertion reactions are predicted where the intrinsic electrochemical stability is smaller than the formation energy toward the most favorable decomposition products. Moreover, these materials can be structurally stable outside the electrochemical stability window. A better understanding of the realistic electrochemical stability window of solid electrolytes helps experimentalists analyze and design new types of solid-state batteries. Stable interfaces and fundamental knowledge about the reactions involved remains of key importance in improving the rate capability and capacity retention in solid-state batteries.

ASSOCIATED CONTENT

Supporting Information

The Supporting Information is available free of charge at https://pubs.acs.org/doi/10.1021/jacsau.1c00228.

Materials, structures, parameters, and a flow diagram used for the density functional theory simulations; metastable phases and corresponding volume, band gap, ionic conductivity, convex hulls and radial distribution functions of solid electrolyte materials (PDF)

AUTHOR INFORMATION

Corresponding Author

Marnix Wagemaker − *Storage of Electrochemical Energy, Department of Radiation Science and Technology, Faculty of*

https://doi.org/10.1021/jacsau.1c00228
JACS Au 2021, 1, 1488−1496

Applied Sciences, Delft University of Technology, Delft 2929JB, The Netherlands; orcid.org/0000-0003-3851-1044; Email: m.wagemaker@tudelft.nl

Authors

Tammo K. Schwietert − *Storage of Electrochemical Energy, Department of Radiation Science and Technology, Faculty of Applied Sciences, Delft University of Technology, Delft 2929JB, The Netherlands*

Alexandros Vasileiadis − *Storage of Electrochemical Energy, Department of Radiation Science and Technology, Faculty of Applied Sciences, Delft University of Technology, Delft 2929JB, The Netherlands*

Complete contact information is available at: https://pubs.acs.org/10.1021/jacsau.1c00228

Author Contributions

All authors have given approval to the final version of the manuscript.

Notes

The authors declare no competing financial interest.

■ ACKNOWLEDGMENTS

Financial support is greatly acknowledged from The Netherlands Organization for Scientific Research (NWO) under VICI grant 16122 and from the eScience Centre and NWO under the joint CSER and eScience programme for Energy Research grant 680.91.087.

■ REFERENCES

(1) Janek, J.; Zeier, W. G. A Solid Future for Battery Development. *Nat. Energy* **2016**, *1* (9), 16141.
(2) Zheng, F.; Kotobuki, M.; Song, S.; Lai, M. O.; Lu, L. Review on Solid Electrolytes for All-Solid-State Lithium-Ion Batteries. *J. Power Sources* **2018**, *389*, 198−213.
(3) Xiao, Y.; Wang, Y.; Bo, S.-H.; Kim, J. C.; Miara, L. J.; Ceder, G. Understanding Interface Stability in Solid-State Batteries. *Nat. Rev. Mater.* **2020**, *5*, 105.
(4) Zhang, Z.; Shao, Y.; Lotsch, B.; Hu, Y.-S.; Li, H.; Janek, J.; Nazar, L. F.; Nan, C.-W.; Maier, J.; Armand, M.; Chen, L. New Horizons for Inorganic Solid State Ion Conductors. *Energy Environ. Sci.* **2018**, *11* (8), 1945−1976.
(5) Yu, C.; Ganapathy, S.; van Eck, E. R. H.; Wang, H.; Basak, S.; Li, Z.; Wagemaker, M. Accessing the Bottleneck in All-Solid State Batteries, Lithium-Ion Transport over the Solid-Electrolyte-Electrode Interface. *Nat. Commun.* **2017**, *8* (1), 1086.
(6) Famprikis, T.; Canepa, P.; Dawson, J. A.; Islam, M. S.; Masquelier, C. Fundamentals of Inorganic Solid-State Electrolytes for Batteries. *Nat. Mater.* **2019**, *18* (12), 1278−1291.
(7) Schwietert, T. K.; Arszelewska, V. A.; Wang, C.; Yu, C.; Vasileiadis, A.; de Klerk, N. J. J.; Hageman, J.; Hupfer, T.; Kerkamm, I.; Xu, Y.; van der Maas, E.; Kelder, E. M.; Ganapathy, S.; Wagemaker, M. Clarifying the Relationship between Redox Activity and Electrochemical Stability in Solid Electrolytes. *Nat. Mater.* **2020**, *19* (4), 428−435.
(8) Zhu, Y.; He, X.; Mo, Y. Origin of Outstanding Stability in the Lithium Solid Electrolyte Materials: Insights from Thermodynamic Analyses Based on First-Principles Calculations. *ACS Appl. Mater. Interfaces* **2015**, *7* (42), 23685−23693.
(9) Richards, W. D.; Miara, L. J.; Wang, Y.; Kim, J. C.; Ceder, G. Interface Stability in Solid-State Batteries. *Chem. Mater.* **2016**, *28* (1), 266−273.
(10) Han, F.; Zhu, Y.; He, X.; Mo, Y.; Wang, C. Electrochemical Stability of $Li_{10}GeP_2S_{12}$ and $Li_7La_3Zr_2O_{12}$ Solid Electrolytes. *Adv. Energy Mater.* **2016**, *6* (8), 1501590.
(11) Han, F.; Gao, T.; Zhu, Y.; Gaskell, K. J.; Wang, C. A Battery Made from a Single Material. *Adv. Mater.* **2015**, *27* (23), 3473−3483.
(12) Tian, Y.; Shi, T.; Richards, W. D.; Li, J.; Kim, J. C.; Bo, S.-H.; Ceder, G. Compatibility Issues between Electrodes and Electrolytes in Solid-State Batteries. *Energy Environ. Sci.* **2017**, *10* (5), 1150−1166.
(13) Perdew, J. P.; Burke, K.; Wang, Y. Generalized Gradient Approximation for the Exchange-Correlation Hole of a Many-Electron System. *Phys. Rev. B: Condens. Matter Mater. Phys.* **1996**, *54* (23), 16533−16539.
(14) Kresse, G.; Hafner, J. *Ab Initio* Molecular Dynamics for Liquid Metals. *Phys. Rev. B: Condens. Matter Mater. Phys.* **1993**, *47* (1), 558−561.
(15) Aydinol, M. K.; Kohan, A. F.; Ceder, G. Ab Initio Calculation of the Intercalation Voltage of Lithium-Transition-Metal Oxide Electrodes for Rechargeable Batteries. *J. Power Sources* **1997**, *68* (2), 664−668.
(16) Jain, A.; Ong, S. P.; Hautier, G.; Chen, W.; Richards, W. D.; Dacek, S.; Cholia, S.; Gunter, D.; Skinner, D.; Ceder, G.; Persson, K. A. Commentary: The Materials Project: A Materials Genome Approach to Accelerating Materials Innovation. *APL Mater.* **2013**, *1* (1), 011002.
(17) Asano, T.; Sakai, A.; Ouchi, S.; Sakaida, M.; Miyazaki, A.; Hasegawa, S. Solid Halide Electrolytes with High Lithium-Ion Conductivity for Application in 4 V Class Bulk-Type All-Solid-State Batteries. *Adv. Mater.* **2018**, *30* (44), 1803075.
(18) Takahashi, K.; Hattori, K.; Yamazaki, T.; Takada, K.; Matsuo, M.; Orimo, S.; Maekawa, H.; Takamura, H. All-Solid-State Lithium Battery with LiBH4 Solid Electrolyte. *J. Power Sources* **2013**, *226*, 61−64.
(19) Teranishi, T.; Ishii, Y.; Hayashi, H.; Kishimoto, A. Lithium Ion Conductivity of Oriented Li0.33La0.56TiO3 Solid Electrolyte Films Prepared by a Sol−Gel Process. *Solid State Ionics* **2016**, *284*, 1−6.
(20) Hakari, T.; Nagao, M.; Hayashi, A.; Tatsumisago, M. All-Solid-State Lithium Batteries with Li3PS4 Glass as Active Material. *J. Power Sources* **2015**, *293*, 721−725.
(21) Zhang, W.; Schröder, D.; Arlt, T.; Manke, I.; Koerver, R.; Pinedo, R.; Weber, D. A.; Sann, J.; Zeier, W. G.; Janek, J. (Electro)Chemical Expansion during Cycling: Monitoring the Pressure Changes in Operating Solid-State Lithium Batteries. *J. Mater. Chem. A* **2017**, *5* (20), 9929−9936.
(22) Fitzhugh, W.; Wu, F.; Ye, L.; Su, H.; Li, X. Strain-Stabilized Ceramic-Sulfide Electrolytes. *Small* **2019**, *15* (33), 1901470.
(23) Park, C.-M.; Sohn, H.-J. Black Phosphorus and Its Composite for Lithium Rechargeable Batteries. *Adv. Mater.* **2007**, *19* (18), 2465−2468.
(24) Boulineau, S.; Tarascon, J.-M.; Leriche, J.-B.; Viallet, V. Electrochemical Properties of All-Solid-State Lithium Secondary Batteries Using Li-Argyrodite Li6PS5Cl as Solid Electrolyte. *Solid State Ionics* **2013**, *242*, 45−48.
(25) Kamaya, N.; Homma, K.; Yamakawa, Y.; Hirayama, M.; Kanno, R.; Yonemura, M.; Kamiyama, T.; Kato, Y.; Hama, S.; Kawamoto, K.; Mitsui, A. A Lithium Superionic Conductor. *Nat. Mater.* **2011**, *10* (9), 682−686.
(26) Lacivita, V.; Wang, Y.; Bo, S.-H.; Ceder, G. *Ab Initio* Investigation of the Stability of Electrolyte/Electrode Interfaces in All-Solid-State Na Batteries. *J. Mater. Chem. A* **2019**, *7* (14), 8144−8155.
(27) Put, B.; Vereecken, P. M.; Stesmans, A. On the Chemistry and Electrochemistry of LiPON Breakdown. *J. Mater. Chem. A* **2018**, *6* (11), 4848−4859.
(28) Yu, X.; Bates, J. B.; Jellison, G. E.; Hart, F. X. A Stable Thin-Film Lithium Electrolyte: Lithium Phosphorus Oxynitride. *J. Electrochem. Soc.* **1997**, *144* (2), 524−532.
(29) Wang, W.; Yue, X.; Meng, J.; Wang, J.; Wang, X.; Chen, H.; Shi, D.; Fu, J.; Zhou, Y.; Chen, J.; Fu, Z. Lithium Phosphorus Oxynitride as an Efficient Protective Layer on Lithium Metal Anodes for Advanced Lithium-Sulfur Batteries. *Energy Storage Mater.* **2019**, *18*, 414−422.

(30) Schwöbel, A.; Hausbrand, R.; Jaegermann, W. Interface Reactions between LiPON and Lithium Studied by In-Situ X-Ray Photoemission. *Solid State Ionics* **2015**, *273*, 51−54.
(31) Schwietert, T.; Arszelewska, V.; Yu, C.; Wang, C. The Relationship between the Redox Activity and Electrochemical Stability of Solid Electrolytes for Solid-State Batteries. *arXiv*, August 27, 2019; arXiv:1908.10144.
(32) Jalem, R.; Morishita, Y.; Okajima, T.; Takeda, H.; Kondo, Y.; Nakayama, M.; Kasuga, T. Experimental and First-Principles DFT Study on the Electrochemical Reactivity of Garnet-Type Solid Electrolytes with Carbon. *J. Mater. Chem. A* **2016**, *4* (37), 14371−14379.
(33) Bohnke, O. Mechanism of Ionic Conduction and Electrochemical Intercalation of Lithium into the Perovskite Lanthanum Lithium Titanate. *Solid State Ionics* **1996**, *91* (1−2), 21−31.
(34) Arbi, K.; Kuhn, A.; Sanz, J.; García-Alvarado, F. Characterization of Lithium Insertion into NASICON-Type Li[Sub 1+x]Ti-[Sub 2-x]Al[Sub x](PO[Sub 4])[Sub 3] and Its Electrochemical Behavior. *J. Electrochem. Soc.* **2010**, *157* (6), A654.
(35) Arbi, K.; Hoelzel, M.; Kuhn, A.; García-Alvarado, F.; Sanz, J. Local Structure and Lithium Mobility in Intercalated Li $_3$ Al $_x$ Ti $_{2-x}$ (PO $_4$) $_3$ NASICON Type Materials: A Combined Neutron Diffraction and NMR Study. *Phys. Chem. Chem. Phys.* **2014**, *16* (34), 18397−18405.
(36) Liang, J.-Y.; Zeng, X.-X.; Zhang, X.-D.; Wang, P.-F.; Ma, J.-Y.; Yin, Y.-X.; Wu, X.-W.; Guo, Y.-G.; Wan, L.-J. Mitigating Interfacial Potential Drop of Cathode−Solid Electrolyte via Ionic Conductor Layer To Enhance Interface Dynamics for Solid Batteries. *J. Am. Chem. Soc.* **2018**, *140* (22), 6767−6770.
(37) Han, F.; Westover, A. S.; Yue, J.; Fan, X.; Wang, F.; Chi, M.; Leonard, D. N.; Dudney, N. J.; Wang, H.; Wang, C. High Electronic Conductivity as the Origin of Lithium Dendrite Formation within Solid Electrolytes. *Nat. Energy* **2019**, *4* (3), 187−196.
(38) Koerver, R.; Zhang, W.; de Biasi, L.; Schweidler, S.; Kondrakov, A. O.; Kolling, S.; Brezesinski, T.; Hartmann, P.; Zeier, W. G.; Janek, J. Chemo-Mechanical Expansion of Lithium Electrode Materials − on the Route to Mechanically Optimized All-Solid-State Batteries. *Energy Environ. Sci.* **2018**, *11* (8), 2142−2158.
(39) Sun, W.; Dacek, S. T.; Ong, S. P.; Hautier, G.; Jain, A.; Richards, W. D.; Gamst, A. C.; Persson, K. A.; Ceder, G. The Thermodynamic Scale of Inorganic Crystalline Metastability. *Sci. Adv.* **2016**, *2* (11), No. e1600225.
(40) Koerver, R.; Walther, F.; Aygün, I.; Sann, J.; Dietrich, C.; Zeier, W. G.; Janek, J. Redox-Active Cathode Interphases in Solid-State Batteries. *J. Mater. Chem. A* **2017**, *5* (43), 22750−22760.
(41) Hakari, T.; Deguchi, M.; Mitsuhara, K.; Ohta, T.; Saito, K.; Orikasa, Y.; Uchimoto, Y.; Kowada, Y.; Hayashi, A.; Tatsumisago, M. Structural and Electronic-State Changes of a Sulfide Solid Electrolyte during the Li Deinsertion−Insertion Processes. *Chem. Mater.* **2017**, *29* (11), 4768−4774.
(42) Kato, Y.; Hori, S.; Saito, T.; Suzuki, K.; Hirayama, M.; Mitsui, A.; Yonemura, M.; Iba, H.; Kanno, R. High-Power All-Solid-State Batteries Using Sulfide Superionic Conductors. *Nat. Energy* **2016**, *1* (4), 16030.

https://doi.org/10.1021/jacsau.1c00228
JACS Au 2021, 1, 1488−1496